Molecular Biology of the Cell
Vol. 20, 4303–4312, October 15, 2009

Retrograde Shiga Toxin Trafficking Is Regulated by ARHGAP21 and Cdc42

Heidi Hehnly,* Katrina Marie Longhini,* Ji-Long Chen,†‡ and Mark Stamnes*

*Department of Molecular Physiology and Biophysics, and †Department of Internal Medicine, Roy J. and Lucille A. Carver College of Medicine, The University of Iowa, Iowa City, IA 52242

Submitted February 25, 2009; Revised August 4, 2009; Accepted August 11, 2009
Monitoring Editor: Adam Linstedt

Shiga-toxin–producing *Escherichia coli* remain a food-borne health threat. Shiga toxin is endocytosed by intestinal epithelial cells and transported retrogradely through the secretory pathway. It is ultimately translocated to the cytosol where it inhibits protein translation. We found that Shiga toxin transport through the secretory pathway was dependent on the cytoskeleton. Recent studies reveal that Shiga toxin activates signaling pathways that affect microtubule reassembly and dynein-dependent motility. We propose that Shiga toxin alters cytoskeletal dynamics in a way that facilitates its transport through the secretory pathway. We have now found that Rho GTPases regulate the endocytosis and retrograde motility of Shiga toxin. The expression of RhoA mutants inhibited endocytosis of Shiga toxin. Constitutively active Cdc42 or knockdown of the Cdc42-specific GAP, ARHGAP21, inhibited the transport of Shiga toxin to the juxtanuclear Golgi apparatus. The ability of Shiga toxin to stimulate microtubule-based transferrin transport also required Cdc42 and ARHGAP21 function. Shiga toxin addition greatly decreases the levels of active Cdc42-GTP in an ARHGAP21-dependent manner. We conclude that ARHGAP21 and Cdc42-based signaling regulates the dynein-dependent retrograde transport of Shiga toxin to the Golgi apparatus.

INTRODUCTION

Enteritis caused by *Shigella* dysenteria and pathogenic strains of *Escherichia coli* is a global health threat. These bacteria secrete Shiga toxin that enters intestinal epithelial cells and kills them by blocking translation. In some cases, the toxin escapes the gut and targets the kidney and vascular endothelium resulting in hemolytic-uremic syndrome (Sandvig and van Deurs, 2000; O'Loughlin and Robins-Browne, 2001; Proulx *et al.*, 2001; Desch and Motto, 2007). Treatment options for *Escherichia coli* infection and hemolytic-uremic syndrome are limited in part because of an incomplete understanding of the molecular mechanisms underlying Shiga toxin's trafficking within cells.

Shiga toxin reaches the cytosol by using retrograde transport through the secretory pathway (Sandvig and van Deurs, 2002; Johannes and Popoff, 2008). Shiga toxin is a heteromultimeric protein containing one A subunit and five B subunits. The A subunit is an *N*-glycosidase that inhibits protein translation, whereas the Shiga toxin B subunits (STxBs) mediate intracellular targeting. STxB binds to the cell surface via a glycolipid receptor, globotriaosyl ceramide (Gb3). Entry is mediated by clathrin-dependent or -independent endocytosis (Lingwood, 1993; Sandvig and van Deurs, 2000). It is transported from early endosomes to the Golgi complex before undergoing COPI-independent retrograde transport to the endoplasmic reticulum (Mallard *et al.*, 1998; Girod *et al.*, 1999; Falguieres *et al.*, 2001; Luna *et al.*, 2002; Lauvrak *et al.*, 2004; McKenzie *et al.*, 2009). The A subunit exits the endoplasmic reticulum into the cytosol where it cleaves the rRNA (Obrig *et al.*, 1985).

Shiga toxin usurps several components of the constitutive trafficking machinery to undergo retrograde transport. Clathrin, clathrin adaptors, EHD3, and the retromer complex are each required during transport from endosomes to the Golgi apparatus (Lauvrak *et al.*, 2004; Bujny *et al.*, 2007; Popoff *et al.*, 2007; Naslavsky *et al.*, 2009). Specific v- and t-SNARES are implicated in membrane fusion events that occur during retrograde toxin trafficking (Mallard *et al.*, 2002; Tai *et al.*, 2004). Also, multiple small GTP-binding proteins are involved in the docking and fusion of toxin containing carriers including Rab6a′, Rab11, Rab43, and Arl1 (Wilcke *et al.*, 2000; Monier *et al.*, 2002; Tai *et al.*, 2005; Fuchs *et al.*, 2007). A recent study revealed that retrograde Shiga toxin transport requires the ARF1-specific guanine-nucleotide-exchange factor, GBF1 (Saenz *et al.*, 2009). We have found previously that the microtubule (MT) cytoskeleton and the minus-end–directed MT motor-protein dynein are required for Shiga toxin's motility from dispersed endosomes to the juxtanuclear Golgi compartment (Hehnly *et al.*, 2006).

Recent studies are revealing that Shiga toxin not only uses the constitutive cellular trafficking machinery but also alters this machinery to influence intracellular transport (Johannes and Popoff, 2008). After binding Gb3, STxB actively tubulates the plasma membrane in a manner that facilitates its endocytosis (Romer *et al.*, 2007). At the time of its entry, STxB activates several protein kinases including Syk, p38, and Cδ (Lauvrak *et al.*, 2006; Torgersen *et al.*, 2007; Walchli *et*

This article was published online ahead of print in *MBC in Press* (http://www.molbiolcell.org/cgi/doi/10.1091/mbc.E09–02–0155) on August 19, 2009.

‡Present address: CAS Key Laboratory of Pathogenic Microbiology and Immunology, Institute of Microbiology, Chinese Academy of Sciences (CAS), Beijing 100101, China.

Address correspondence to: Mark Stamnes (mark-stamnes@uiowa.edu).

Abbreviations used: ARF1, ADP-ribosylation factor; Gb3, globotriaosyl ceramide; MT, microtubule; STxB, Shiga toxin B subunit.

al., 2008). Protein kinase Cδ and p38 are required for transport into the Golgi apparatus (Torgersen *et al.*, 2007; Walchli *et al.*, 2008). The activation of Syk results in clathrin heavy-chain phosphorylation and an increase in the clathrin-dependent endocytosis of STxB (Lauvrak *et al.*, 2006). Although the toxin-dependent signaling pathways mostly involve the B subunit, the A subunit can also stimulate clathrin-dependent endocytosis through an unknown mechanism (Torgersen *et al.*, 2005). It is likely that Shiga toxin utilizes intracellular signaling to regulate its entry into target cells.

In addition to activating endocytosis, Shiga toxin may influence signaling important for later trafficking events. After Shiga toxin binds to the cell surface, there is an increase in MT assembly and the number of microfilaments (Takenouchi *et al.*, 2004). STxB stimulates dynein-based motility that may facilitate its own transport to the juxtanuclear Golgi apparatus (Hehnly *et al.*, 2006). There was an increase in neurotransmitter release in mice treated intraperitoneally with Shiga toxin. These mice displayed cytoskeletal remodeling in the lumbar motoneuron, suggesting that Shiga toxin can influence cytoskeleton dynamics leading to changes in the intracellular trafficking of synaptic vesicles (Obata *et al.*, 2008). The signaling events that connect Shiga toxin entry to the change in cytoskeletal dynamics are poorly understood.

The Arf, Rab, and Rho families of small Ras-like GTP-binding proteins are candidates for connecting protein transport to cytoskeletal dynamics. The three best-characterized Rho-family members, Cdc42, RhoA, and Rac1, regulate various aspects of membrane trafficking (Etienne-Manneville and Hall, 2002; Sabharanjak *et al.*, 2002; Hall, 2005; Malyukova *et al.*, 2009). Cdc42 and Cdc42-like proteins, TCL and TC10, are regulators of the early endocytic pathway (Chiang *et al.*, 2001; de Toledo *et al.*, 2003). Cdc42 and a Cdc42-specific GTPase-activating protein (GAP), ARHGAP21 (also referred to as ARHGAP10) are required for clathrin-independent endocytosis of glycosylphosphatidylinositol (GPI)-anchored proteins (Sabharanjak *et al.*, 2002; Kumari and Mayor, 2008). Recent studies revealed that Cdc42 regulates ARF1-dependent intracellular trafficking events. First, ARHGAP21 binds directly to ARF1 (Dubois *et al.*, 2005; Menetrey *et al.*, 2007). Second, Cdc42 binding to Golgi membranes requires an interaction with the ARF1-dependent vesicle coat protein coatomer (Wu *et al.*, 2000; Fucini *et al.*, 2002). We have previously reported that coatomer-bound Cdc42 regulates dynein recruitment at the Golgi apparatus (Chen *et al.*, 2005).

Given that Rho GTPases are known regulators of cytoskeletal dynamics and that the cytoskeleton mediates Shiga toxin motility from the cell periphery to the juxtanuclear Golgi compartment (Hehnly *et al.*, 2006), we investigated the contribution of Rho GTPases to Shiga toxin's retrograde transport. Here, we present evidence that RhoA regulates the internalization of STxB, whereas Cdc42 regulates the motility of STxB to the juxtanuclear Golgi apparatus. Interestingly, STxB addition greatly decreases the levels of active Cdc42. We found that Cdc42 and ARHGAP21 signaling is required for the dynein-dependent motility of STxB and for the ability of STxB to stimulate MT-based intracellular trafficking.

MATERIALS AND METHODS

The following antibodies were used: mouse anti-myc (Sigma-Aldrich, St. Louis, MO), rabbit anti-Cdc42 (Cell Signaling, Beverly, MA), mouse anti-GM130 (BD Biosciences, San Jose, CA), rabbit anti-giantin (Covance, Madison, WI), rabbit anti-N-WASP (Cytoskeleton, Denver, CO), Alexa Fluor 647 goat anti-mouse and goat anti-rabbit, and Alexa Fluor 488 goat anti-rabbit. Alexa Fluor 594– and 647–conjugated transferrin and NBD C_6-ceramide were obtained from Invitrogen (Carlsbad, Ca). Nocodazole, *Clostridium difficile* toxin B, and cytochalasin D were obtained from Sigma-Aldrich.

Preparation of Recombinant STxB

STxB containing a C-terminal His-tag was cloned into the pET11a vector (Stratagene, La Jolla, CA). STxB-His was expressed in BL21(DE3)pLysS bacterial strain (Stratagene) and purified on nickel beads by using a 20–500 mM continuous imidazole gradient. STxB was labeled using Cy3.5 (GE Healthcare, Waukesha, WI) for fluorescence microscopy (Hehnly *et al.*, 2006).

Immunofluorescence

Immunofluorescence was performed as described previously (Hehnly *et al.*, 2006). Images were acquired using a confocal microscope (model LSM-510; Carl Zeiss MicroImaging, Thornwood, NY) and a 63× objective (Carl Zeiss MicroImaging) with an NA of 1.40.

Vero Cell–based Trafficking Assays

African green monkey kidney (Vero) cells were cultured in α-minimal essential medium (MEM) supplemented with 10% fetal bovine serum (FBS) and 100 U/ml penicillin-streptomycin. Vero cells were grown to subconfluence on glass coverslips. Cells were transfected using Lipofectamine 2000 (Invitrogen) with plasmids expressing myc-Cdc42, GFP-RhoA(T19N), GFP-RhoA(G14V), GFP-Rac1(T17N), GFP-Rac1(G12V), GFP-Cdc42(Q61L), GFP-Cdc42(T17N), or green fluorescent protein (GFP). Cells were incubated on ice with 2.5 μg/ml STxB in α-MEM without 10% FBS for 2 min. The cells were washed three times with fresh medium and incubated at 37°C for various times as described in the figure legends with α-MEM supplemented with 10% FBS (Hehnly *et al.*, 2006). The media was supplemented with 100 ng/ml toxin B or vehicle. The cells were pretreated for 1 h with Toxin B before addition of STxB (see Figure 2).

When assaying transferrin localization, subconfluent Vero cells were starved of serum for 1 h before the addition of 200 μg/ml Alexa Fluor 647–conjugated transferrin. Cells were treated with or without 2.5 μg/ml STxB. Transferrin and STxB were bound on ice for 5 min. The cells were washed with fresh medium and placed at 37°C. The warmed medium was then removed, and 37°C α-MEM medium plus 100 μg/ml unlabeled transferrin was added to the cells. The medium was removed after 30 min, and the cells were fixed with 4% paraformaldehyde (PFA) (Hehnly *et al.*, 2006).

Quantification of STxB Localization

Images were captured in tiff format using the LSM-510 confocal microscope (Zeiss). Using Adobe Photoshop (San Jose, CA) total internalized fluorescence of STxB was measured by outlining the entire cell (see Figure 3, Supplemental Figures S4 and S5). The total fluorescence for STxB was measured by multiplying the mean intensity by the total number of pixels in the selected area. Quantification of juxtanuclear localized STxB in the presence of toxin B was done by scoring cells in a blind manner. P values were assessed using Student's *t* test. To calculate the percent of STxB at the Golgi apparatus, we outlined the GM130-labeled Golgi apparatus and the entire cell. The percent fluorescence of STxB at the Golgi apparatus compared with total STxB fluorescence was then calculated for each cell. For each experiment, 7–20 cells were randomly selected for each variable. P values were calculated using Student's *t* tests.

Time-Lapse Confocal Microscopy

The Golgi apparatus was labeled in Vero cells by incubating them with 5 μM NBD C6-ceramide–bovine serum albumin complex for 30 min at 4°C. The cells were rinsed three times with fresh α-MEM and incubated at 37°C for 30 min. The cells were incubated with STxB for 10 s at 37°C and rinsed three times with fresh medium. They were then incubated in a bicarbonate-free medium containing 1 mM magnesium acetate, 1 mM $CaCl_2$, 5 mM glucose, 1× phosphate-buffered saline (PBS), 5 mM glutamate, 1 mM sodium pyruvate, and 10% FBS. Imaging was performed using an LSM-510 inverted confocal microscope with a heated stage, and images were captured with a 40× oil immersion objective (Zeiss). Kinetic analysis of Cy3.5-labeled STxB arrival at the Golgi apparatus was accomplished by measuring fluorescence changes in a defined region of interest (ROI) by using Zeiss LSM software (Hehnly *et al.*, 2006).

shRNA-based Depletion of ARHGAP21 in Vero Cells

The pSUPER RNAi System (Oligoengine, Seattle, WA) was used to generate a viral vector pSR-shARHGAP21 to produce an shRNA to ARHGAP21. The oligonucleotides used for the shRNA were 5′-GATCCCCGTCATTGTGCCTTCTGAGATTCAAGAGATCTCAGAAGGCACAATGACTTTTTGGAAA-3′ and 5′AGCTTTTCCAAAAAGTCATTGTGCCTTCTCAGAATCTCTTGAATCTCAGAAGGCACAATGACGGG-3′ (Kumari and Mayor, 2008). The oligonucleotide duplex was cloned into pSRgfp/neo by BglII/HindIII sites. A stable cell line expressing the shRNA to ARHGAP21 was generated using a retroviral spin infection. Retroviral supernatant was generated from 293T cells transfected with the pSR-shARHGAP21 with the pCL-Eco packaging construct and pCL-VSVG. Vero cells were grown to subconfluence in a 12-well dish. Cells and

viral supernatant were centrifuged at 2500 r.p.m. for 2 h at 32°C with 8 μg/ml polybrene. Several clonal populations of GFP- expressing cells were obtained and measured for ARHGAP21 depletion. To measure ARHGAP21 depletion a short-length (< 1 kb) cDNA library was generated from total RNA by using the Aurum total RNA mini kit (Bio-Rad, Hercules, CA) and iScript cDNA Synthesis kit (Bio-Rad, Hercules, CA). ARHGAP21 primers, position 2390–2413 and position 2539–2516, were used for quantitative real-time PCR. Primers targeting the ARHGAP21 intron, actin, and GAPDH were used as controls. Primer sequences are available upon request. SYBR green supermix, MyiQ single-color PCR detection system, and optical system software (Bio-Rad) were used for real-time PCR (Pfaffl, 2001). For the rescue experiment, the ARHGAP21 cell line was transfected with an ARHGAP21(aa 855-1346)-mCherry that is missing the siRNA target site.

Cdc42 Activation Assay

Glutathione *S*-transferase (GST)-p21-binding domain (PBD) was expressed in BL21 cells (Stratagene). The bacteria were lysed and GST-PBD protein was isolated on glutathione Sepharose 4B (GE Healthcare). Vero cells with or without a short hairpin RNA (shRNA) to ARHGAP21 were transfected with myc-Cdc42. Forty-eight hours after the transfection, the cells were treated with or without STxB and incubated at 37°C for 20 min. The cells were harvested, rinsed in PBS, and lysed in ice-cold radioimmunoprecipitation assay (RIPA) buffer (50 mM Tris-HCl, pH 7.2, 150 mM NaCl, 10 mM $MgCl_2$, 0.5% sodium deoxycholate, 1% Triton X-100, 0.1% SDS, 0.5 mM Na_3VO_4, 15 μg/ml leupeptin, 5 μg/ml aprotinin 1 μg/ml pepstatin A, and 1 μM PMSF). The lysates were incubated with GST-PBD beads at 4°C for 45 min. The beads were washed three times with ice-cold wash buffer (50 mM Tris-HCl, pH 7.2, 150 mM NaCl, 10 mM $MgCl_2$, 1% Triton X-100, 15 μg/ml leupeptin, 5 μg/ml aprotinin, 1 μg/ml pepstatin A, and 1 μM PMSF). The beads were resuspended in SDS sample buffer, boiled, and processed for SDS-PAGE and Western blotting. The Western blot was probed with mouse anti-myc to detect Cdc42. Where indicated Western blot signals were quantified by densitometry.

RESULTS

The MT and Actin Cytoskeleton Are Required for the Motility of Shiga Toxin to the Juxtanuclear Golgi Region

The total contribution of the cytoskeleton during Shiga toxin transport from the cell surface to the ER is unclear. The role of the actin and MT cytoskeleton during Shiga toxin transport to the Golgi apparatus has been studied using cytoskeletal inhibitors (Mallard *et al.*, 2002; Yoshino *et al.*, 2005). In these experiments, STxB was trapped in a pre-Golgi intracellular compartment using a 19.5°C block. The cells were then shifted to 37°C at which trafficking into the Golgi complex proceeds. Neither MT- nor actin-disrupting drugs, when added after the 19.5°C temperature block, caused an inhibition of trafficking into the Golgi apparatus (Mallard *et al.*, 1998). By contrast, we have reported that dynein motors and MTs are required for STxB transport to the Golgi apparatus when trafficking occurs in the absence of a 19.5°C temperature block (Hehnly *et al.*, 2006). A possible conclusion from this previous work is that STxB transport from the cell surface to the Golgi apparatus involves a cytoskeleton-dependent step that proceeds during a 19.5°C incubation, followed by a cytoskeleton-independent entry step into the Golgi apparatus.

To test this conclusion, we examined if STxB is motile during a 19.5°C incubation. Vero cells were incubated with Cy3.5-tagged STxB for 5 min at 0°C to allow binding to the cell surface. STxB was then allowed to internalize by incubating for 1 h at 19.5°C. We found that at the end of the 19.5°C incubation, most of the STxB is adjacent to, but not fully overlapping with the Golgi apparatus (Figure 1A). The STxB-containing compartment colocalized with the early endosome marker, EEA1 (Supplemental Figure S1). We then shifted the cells to 37°C for 30 min, conditions shown previously to be permissive for entry into the Golgi apparatus (Mallard *et al.*, 2002; Yoshino *et al.*, 2005). When we added the MT toxin nocodazole between the 19.5 and 37°C incubations, we found that there was no change in the amount of juxtanuclear Golgi localized STxB (Figure 1B and Supplemental Figure S2). Similar results were obtained with the actin toxin cytochalasin D (Supplemental Figure S3). This result is consistent with the previously published finding that the cytoskeleton is not required for STxB trafficking from the 19.5°C block compartment to the Golgi complex.

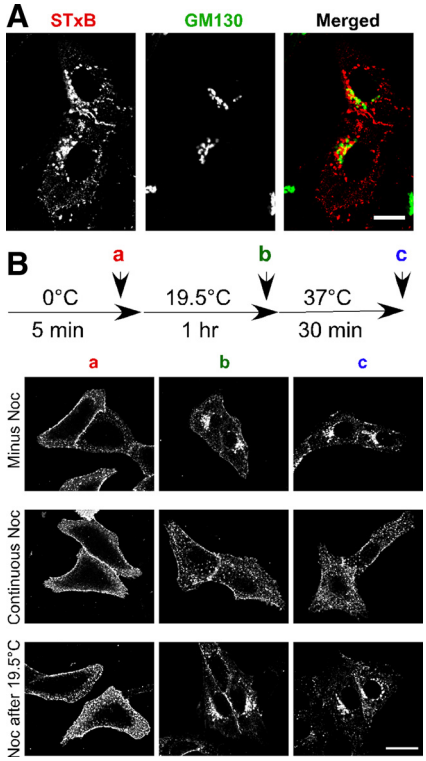

Figure 1. STxB transport to the Golgi apparatus requires MTs. (A) Shown are confocal micrographs of Vero cells incubated with Cy3.5-labeled STxB (red) at 19.5°C for 1 h. The cells were fixed, permeabilized, and labeled with a mouse polyclonal antibody against the Golgi marker GM130 (green). The merged image indicates overlap (yellow) between STxB and GM130. Bar, 10 μm. (B) Vero cells were incubated with STxB at 0, 19.5, and 37°C consecutively as indicated in the diagram. Nocodazole was included during the 0°C incubation or after the 19.5°C incubation as indicated. Cells were fixed after the 0°C (a in diagram), 19.5°C (b in diagram), or the 37°C incubation (c in diagram). Bar, 20 μm.

The results were strikingly different when we disrupted the MTs with nocodazole before the 19.5°C block. In this case, STxB remained dispersed in the cell, both following the 1-h 19.5°C incubation and after the 30-min 37°C incubation (Figure 1B). When actin dynamics were disrupted before the 19.5°C block with cytochalasin D, we observed a reduction in the levels of Golgi-associated STxB (Supplemental Figure S3A). Cytochalasin D also blocks STxB transport to the Golgi apparatus in the absence of a 19.5°C temperature block (Supplemental Figure S3B). We determined the kinetics of STxB trafficking into the juxtanuclear Golgi region by using time-lapse confocal microscopy with living cells. In the absence of cytochalasin D, STxB levels in a defined juxtanuclear region increased linearly (Supplemental Figure S3C). After acute cytochalasin D treatment, the rate of STxB arrival was inhibited. These results are consistent with our previous report (Hehnly *et al.*, 2006) and indicate that both MTs and actin are required for STxB motility from the cell periphery to a juxtanuclear Golgi complex. We conclude that there is a cytoskeleton-dependent motility step that proceeds at 19.5°C. Hence, the 19.5°C temperature block likely

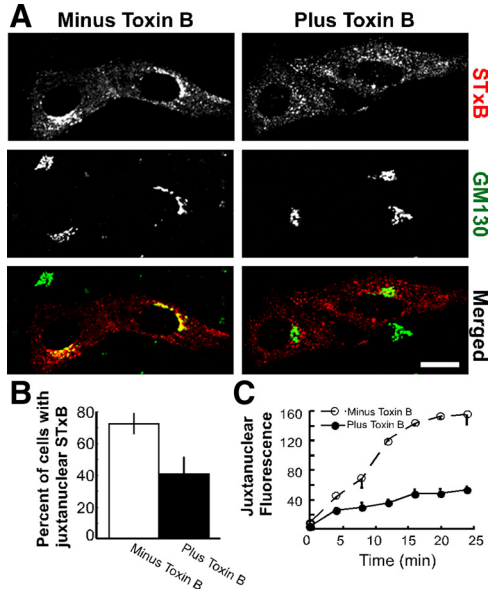

Figure 2. STxB requires Rho-family GTPases for retrograde transport to the Golgi apparatus. (A) Shown are confocal micrographs of Vero cells incubated with Cy3.5-labeled STxB (red) for 30 min. Toxin B was included during the incubation where indicated. The cells were fixed, permeabilized, and labeled with antibodies to the Golgi marker GM130 (green). The merged images indicate the overlap (yellow) between STxB and GM130. Bar, 10 μm. (B) The fraction of cells with juxtanuclear STxB was quantified for three experiments ($n > 50$ cells per sample). Bars, SE. The effect of toxin B on STxB localization was significant, $p < 0.04$. (C) The average intensity of fluorescent STxB present in a circular ROI placed at NBD C6-ceramide labeled Golgi complexes were plotted as a function of time. The cells were pretreated with toxin B (●) or mock-treated (○). The ROI was the same size for each cell imaged. Bars, SE; $n = 3$ experiments.

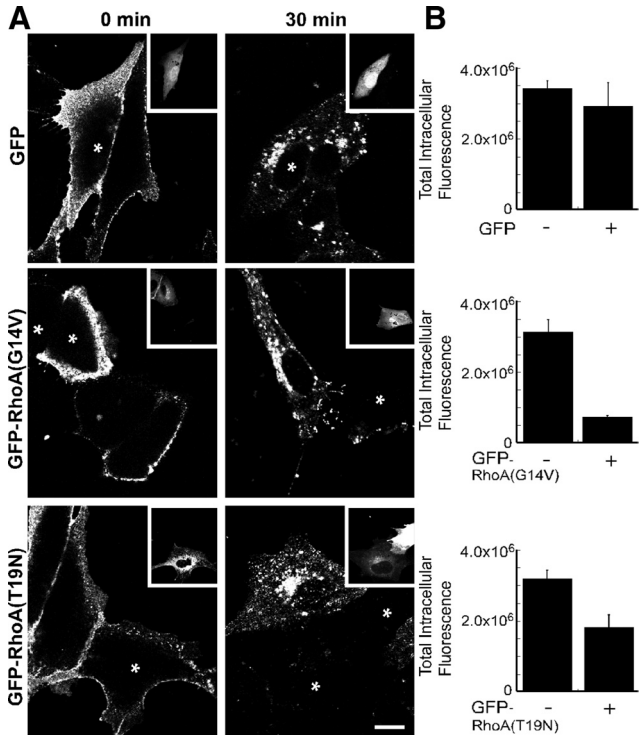

Figure 3. RhoA mutants inhibit the endocytosis of STxB. (A) Shown are confocal micrographs of Vero cells that have been incubated with Cy3.5-labeled STxB for 0 or 30 min as indicated. The cells were transiently transfected with GFP, GFP-RhoA(G14V), or GFP-RhoA(T19N). GFP fluorescence is shown as an inset image and transfected cells are labeled with an asterisk. Bar, 5 μm. (B) GFP, GFP-RhoA(G14V), or GFP-RhoA(T19N) transfected Vero cells were incubated with Cy3.5-labeled STxB for 30 min. The total intracellular fluorescence of STxB was quantified. Bars, SE; $n = 4$ experiments. The effects of RhoA(G14V) ($p < 0.001$) and RhoA(T19N) ($p < 0.02$) were significant when compared with the control. There was no significant difference between GFP and control ($p = 0.53$).

resolves a cytoskeleton-dependent motility step from a cytoskeleton-independent Golgi apparatus entry step.

STxB Requires Rho-family GTPases for Retrograde Transport to the Golgi Apparatus

When Vero cells are incubated with STxB, the rate of MT/dynein-dependent transferrin transport to a juxtanuclear endosome is increased. Concomitantly, there is an increase in the rate of MT polymerization and formation of microfilaments (Takenouchi *et al.*, 2004; Hehnly *et al.*, 2006). The STxB-dependent change in cytoskeletal dynamics may facilitate Shiga-toxin motility to the Golgi apparatus (Hehnly *et al.*, 2006). The molecular mechanism that enables STxB to affect MT-motor–dependent motility and to increase cytoskeleton assembly is unknown. Arp2/3-dependent actin polymerization, MT dynamics, and motor proteins are each regulated by the Rho-family of GTP-binding proteins. Therefore, we examined whether Rho GTPases regulate the MT/dynein-dependent motility of STxB from the cell periphery to the juxtanuclear Golgi region.

Rho-GTPase activity was acutely inhibited in Vero cells using *C. difficile* toxin B. Toxin B glucosylates all members of the Rho family and inhibits their effector interactions (Aktories *et al.*, 2000). In cells treated with toxin B for 30 min, STxB was not transported to the Golgi apparatus and remained dispersed throughout the cell (Figure 2A). By contrast, there is an accumulation of STxB at the juxtanuclear Golgi region by 30 min in untreated cells. The fraction of cells containing juxtanuclear STxB was significantly reduced following toxin B treatment (Figure 2B). Videomicroscopy was used to test the effects of toxin B on STxB motility in live cells. STxB fluorescence in a defined region over the Golgi apparatus increases at a significantly reduced rate in toxin B–treated cells (Figure 2C). We saw no significant decrease in internalized STxB in cells treated with toxin B (Supplemental Figure S4A). We concluded that STxB requires members of the Rho GTPase family for efficient motility to the juxtanuclear Golgi apparatus.

RhoA Inhibits the Endocytosis of STxB

The Rho GTPase family is defined by three subfamilies represented by Rac1, RhoA, and Cdc42 (Etienne-Manneville and Hall, 2002). These proteins cycle between the GTP-(activated) and GDP-bound (inactivated) forms. Because of this cycle, constitutively activating or dominant-negative mutations both can disrupt cellular processes (e.g., Wu *et al.*, 2000; Desai *et al.*, 2004; Hoppe *et al.*, 2006). To test the role of the entire GTP-binding/hydrolysis cycle, we expressed dominant-negative and constitutively active versions of RhoA, Rac1, and Cdc42 and determined their influence on STxB trafficking. We found that the expression of mutant RhoA blocks STxB internalization (Figure 3), but not the initial STxB binding (Supplemental Figure S5). Constitu-

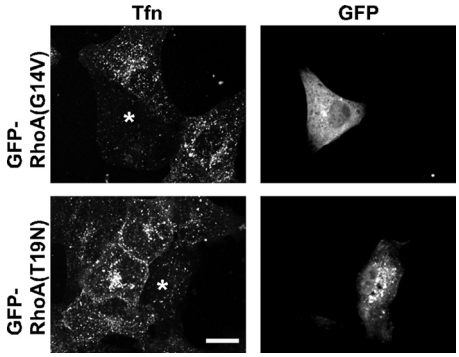

Figure 4. Expression of mutant RhoA inhibits transferrin endocytosis. Shown are confocal micrographs of Vero cells expressing GFP-RhoA(G14V) or GFP-RhoA(T19N). The cells were incubated with transferrin Alexa Fluor 555 conjugate (shown) for 20 min at 37°C. The cells were fixed and mounted for microscopy. Bar, 10 μm.

tively active GFP-RhoA(G14V) reduced the levels of intracellular STxB by fivefold. Expression of dominant-negative GFP-RhoA(T19N) reduced the levels by twofold (Figure 3B). GFP alone had no significant effect on the amount of fluorescent STxB internalized (Figure 3). The consequence of RhoA disruption appeared to be specific because mutant Rac1 and mutant Cdc42 had much smaller effects on STxB internalization. The amount of internalized STxB in either mutant Rac1 or mutant Cdc42 expressing cells was at least 70% of the amount endocytosed into control cells (Supplemental Figure S4, B and C). We concluded that RhoA(T19N) and RhoA(G14V) decreased the endocytosis of STxB.

There could be several explanations for the inhibition of STxB internalization by the expression of mutant RhoA proteins. RhoA could be required directly for endocytosis of STxB. Alternatively, RhoA may influence STxB internalization indirectly by disrupting the distribution of its receptor, Gb3. To distinguish between these possibilities, we compared the localization of STxB in the presence or absence of mutant RhoA. Shortly after adding STxB to the cells, we found that it was localized to the cell surface both in cells expressing mutant forms of RhoA and in control cells. After incubating the cells for 30 min, STxB was internalized and transported to the Golgi apparatus in the control cells. By contrast, little STxB was found in internal compartments (Figure 3A) after 30 min in the presence of mutant RhoA. The observation that STxB still localizes to the cell surface (Supplemental Figure S5), whereas its internalization is inhibited by RhoA mutant expression (Figure 3), suggests that STxB internalization is not solely a consequence of defective Gb3 distribution.

Rho GTPases have been implicated previously in clathrin-dependent endocytosis (Lamaze *et al.*, 1996). Hence, we used receptor-mediated transferrin uptake to determine whether RhoA specifically regulates STxB internalization or acts generally as a regulator of clathrin-based internalization. Cells expressing mutant forms of RhoA internalized less transferrin (Figure 4). Expression of mutant forms of either Rac1 or Cdc42 had no overt effects on the amount of internalized transferrin (Supplemental Figure S6). We conclude that RhoA does not function specifically during STxB endocytosis, but instead acts as a general regulator of clathrin-based endocytosis.

Paradoxically, expressing the mutant forms of RhoA caused a clear inhibition of STxB internalization, but there was no significant defect in STxB endocytosis in cells treated with toxin B (Supplemental Figure S4A). One possibility is

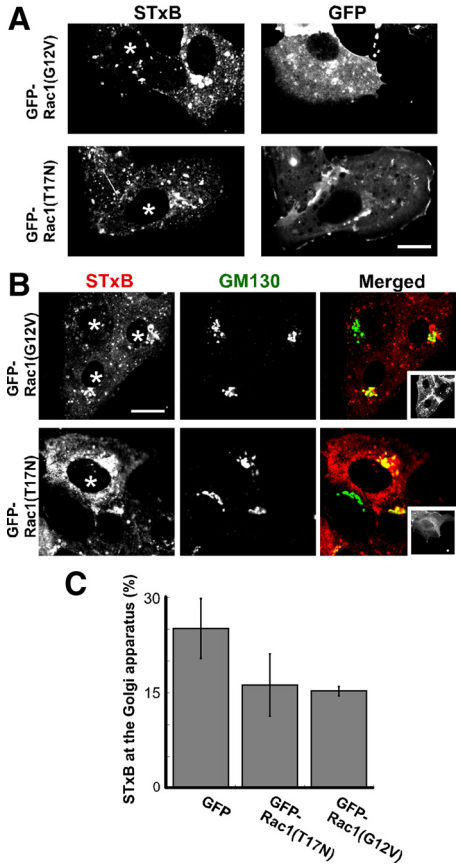

Figure 5. Rac1 has little effect on the accumulation of STxB at the Golgi apparatus. (A) Shown are confocal micrographs of Vero cells incubated with Cy3.5-labeled STxB (left images) for 30 min. The cells were transfected with either GFP-Rac1(G12V) or GFP-Rac1(T17N) as indicated. The GFP fusion protein localization is shown (right images). Transfected cells are also labeled with an asterisk. Bar, 10 μm. (B) GFP-Rac1(G12V) or GFP-Rac1(T17N) expressing cells were incubated with Cy3.5-labeled STxB (red) for 30 min, fixed, permeabilized, and labeled with an antibody against the Golgi marker GM130 (green). The inset images display the GFP-fusion proteins. Bar, 10 μm. (C) Vero cells were incubated with Cy3.5-labeled STxB for 30 min. STxB fluorescence at the Golgi apparatus was quantified as a fraction of the total internalized STxB in cells expressing GFP, GFP-Rac1(G12V), or GFP-Rac1(T17N). Bars, SE; n = 3 experiments. The effect of Rac1(T17N) ($p = 0.26$) or GFP-Rac1(G12V) ($p = 0.11$) was insignificant when compared with GFP alone. There was no significant difference between GFP-Rac1(T17N) and GFP-Rac1(G12V) ($p = 0.86$).

that RhoA function during endocytosis is resistant to toxin B. A more likely possibility is that chronic, but not acute, inhibition of RhoA affects endocytosis. Regardless, the fact that toxin B blocks the subsequent trafficking of internalized Shiga toxin to the Golgi apparatus indicates that there is at least one additional requirement for Rho GTPases.

Rac1 Function Is Not Required for STxB Transport to the Juxtanuclear Golgi

Unlike cells expressing mutant RhoA or treated with toxin B, cells expressing mutant Rac1 were able to internalize STxB (Supplemental Figure S4C) and transport STxB to the juxtanuclear Golgi region (Figure 5, A and B). To determine if there were more subtle defects in STxB trafficking, we quantified the amount of STxB that had arrived at the jux-

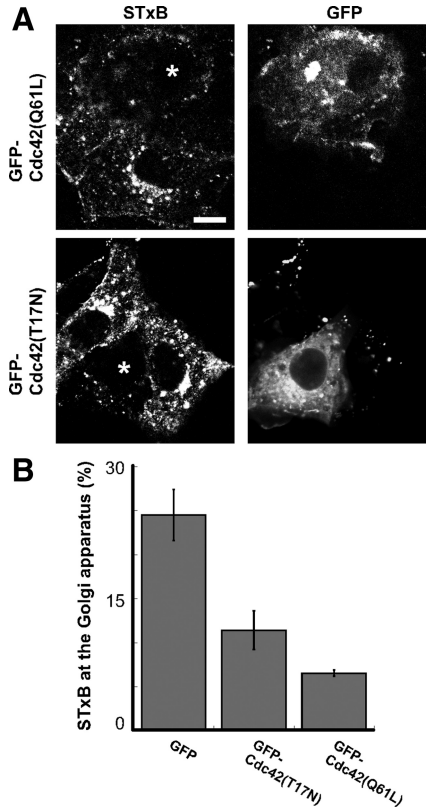

Figure 6. Mutant forms of Cdc42 disrupt STxB transport to the Golgi apparatus. (A) Shown are confocal micrographs of Vero cells expressing either GFP-Cdc42(Q61L) or GFP-Cdc42(T17N) (marked with asterisk) and incubated with Cy3.5-labeled STxB (shown) for 30 min at 37°C. Bar, 10 μm. (B) STxB fluorescence at the Golgi apparatus was quantified as a fraction of the total internalized STxB level in cells expressing GFP, GFP-Cdc42(T17N), or GFP-Cdc42(Q61L). Bars, SE; n = 4 experiments. The effect of GFP-Cdc42(T17N) ($p < 0.02$) and GFP-Cdc42(Q61L) ($p < 0.001$) on STxB levels is significant when compared with GFP alone. There was no significant difference between GFP-Cdc42(T17N) and GFP-Cdc42(Q61L) ($p = 0.10$).

tanuclear Golgi region after 30 min. Golgi apparatus-associated STxB levels were somewhat reduced in cells expressing constitutively active Rac1(G12V) and dominant-negative Rac1(T17N) (Figure 5A and C). Hence, although Rac1 appears to contribute to STxB trafficking, there does not appear to be an absolute requirement for Rac1 function during transport to the Golgi apparatus. Thus, neither RhoA nor Rac1 disruption closely mimicked the consequences of toxin B treatment.

Cdc42 Function is Required for Shiga Toxin Motility to the Juxtanuclear Golgi Apparatus

We found that the expression of constitutively active Cdc42 caused severe disruptions in Shiga toxin trafficking reminiscent of those we observed with toxin B. Very little STxB was observed at the juxtanuclear Golgi apparatus 30 min after STxB addition in cells expressing constitutively active Cdc42(Q61L). Instead, STxB appeared in dispersed punctate structures (Figure 6A). Similar disruptions in STxB trafficking were observed in cells expressing dominant-negative Cdc42(T17N) (Figure 6A). The levels of Golgi-localized STxB was reduced threefold in cells expressing GFP-Cdc42(Q61L) (Figure 6B). Overall, cells expressing dominant-negative Cdc42(T17N) display a twofold decrease in Golgi-associated STxB levels (Figure 6B). However, defects in STxB trafficking were more severe in cells expressing Cdc42(T17N) at a high level. Disrupting Cdc42 expression using previously characterized siRNAs (Deroanne *et al.*, 2005) causes pleiotropic defects in cell morphology, but also has defects in STxB trafficking consistent with expression of Cdc42 mutants (Supplemental Figure S7). The severe defects in STxB transport and the abnormal distribution of STxB into dispersed punctate structures that we observed upon disrupting Cdc42 suggest that Cdc42 is the target of toxin B that affects STxB trafficking.

ARHGAP21 Regulates the Transport of STxB to the Juxtanuclear Golgi

We found that both Cdc42(Q61L) and Cdc42(T17N) inhibit endosome to Golgi apparatus transport. This is reminiscent of ER-to-Golgi apparatus transport in which both the constitutively active and dominant-negative Cdc42 mutants are also inhibitory (Wu *et al.*, 2000). These results suggest that the GTP-binding/hydrolysis cycle is needed for trafficking events toward the Golgi apparatus. With this in mind we sought to examine the effects of disrupting the GTPase cycle of endogenous Cdc42. We did this by inhibiting the expression of the Cdc42-specific GAP, ARHGAP21, which together with ARF1 regulates endocytic and exocytic protein trafficking (Dubois *et al.*, 2005; Kumari and Mayor, 2008).

We generated Vero cells that stably expressed an shRNA targeting ARHGAP21. The sequence used in the shRNA was previously characterized (Kumari and Mayor, 2008). Quantitative RT-PCR analysis revealed that ARHGAP21 transcript levels were reduced 72% in these cells. We examined each of the trafficking steps during STxB internalization to determine if ARHGAP21 function is involved. STxB binding to the cell surface appeared to be normal in ARHGAP21-knockdown cells, indicating that cell-surface Gb3-receptor levels were adequate. STxB internalization was not overtly affected by reduced ARHGAP21 expression (Supplemental Figure S4D). After 30 min, STxB localization in ARHGAP21 shRNA-expressing cells was similar to that observed in cells expressing mutant Cdc42 or treated with toxin B. Specifically, little STxB localized to the juxtanuclear Golgi region and instead was found in dispersed punctate structures (Figure 7A). Clear STxB accumulation at a juxtanuclear Golgi region was observed in control cells not expressing the ARHGAP21 shRNA (Figure 7A). Quantification of STxB levels at the Golgi apparatus confirmed that STxB trafficking was abnormal (Figure 7B). An mCherry-tagged fragment of ARHGAP21 containing the ARF-binding and GAP domains, but devoid of the shRNA target site was expressed in our ARHGAP21 knockdown cell line to confirm that the phenotype of the knockdown cells did not represent an off-target effect (Figure 7C). We found that the ARF-binding and GAP domains of ARHGAP21 were sufficient to restore STxB motility to the Golgi apparatus in knockdown cells. We conclude that the ARHGAP21-regulated pool of Cdc42 is involved in STxB trafficking.

STxB Causes a Decrease in GTP-bound Cdc42

Shiga toxin activates dynein-based motility and possibly other events that influence its intracellular trafficking. Therefore, we were interested in whether Cdc42 mediates these signaling events downstream of STxB. Hence, we examined whether Shiga toxin affects Cdc42 activation. We did this by measuring the levels of myc-tagged Cdc42-GTP bound to the p21-binding domain (PBD) of Pak1 fused to GST (GST-PBD). We found that STxB caused a 10-fold decrease in

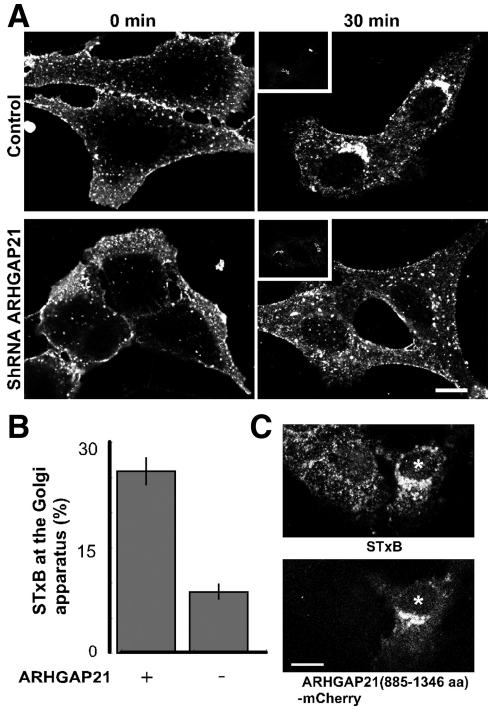

Figure 7. ARHGAP21 shRNA inhibits STxB transport to the juxtanuclear Golgi region. (A) Shown are confocal micrographs of cells stably expressing an shRNA to ARHGAP21 compared with control cells. The cells were incubated with Cy3.5-labeled STxB for either 0 or 30 min and labeled with an antibody against the Golgi marker GM130 (inset). Bar, 10 μm. (B) The cells were incubated with Cy3.5-labeled STxB for 30 min. STxB fluorescence at the Golgi apparatus was quantified as a fraction of total internalized STxB in cells with or without the shRNA to ARHGAP21. Bars, SE; n = 3 experiments. The effect of ARHGAP21 shRNA on STxB levels is significant ($p < 0.02$) when compared with control cells. (C) Shown are confocal micrographs of cells stably expressing an shRNA to ARHGAP21 transiently transfected with ARHGAP21(885-1346 aa)-mCherry. The cells were incubated with Cy3.5-labeled STxB for 30 min. Bar, 10 μm.

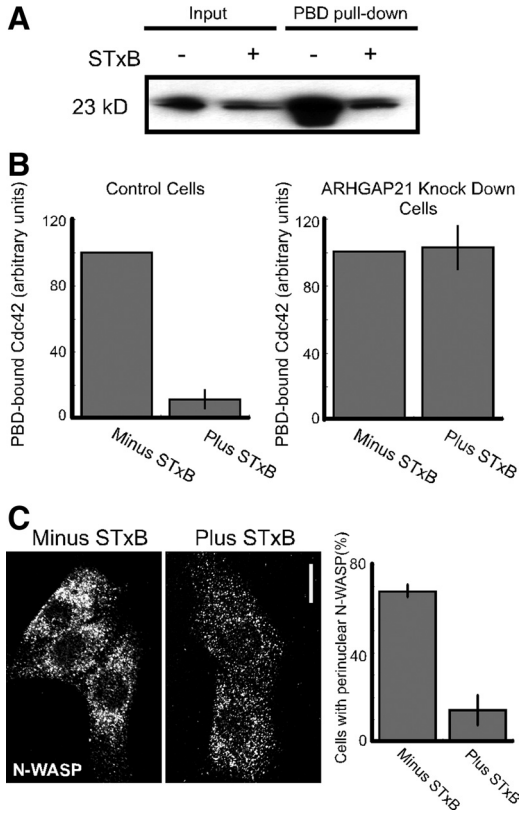

Figure 8. STxB decreases GTP-bound Cdc42 levels. (A) Myc-Cdc42–transfected Vero cell lysates were used for pulldown Cdc42 activation assays with GST-PBD. The cells were incubated with STxB where indicated. Five percent of each lysate and 40% of the bound material were fractionated by SDS-PAGE, electroblotted, and probed with antibodies against the myc epitope. (B) Control Vero cells and cells stably expressing an shRNA to ARHGAP21 were analyzed as in A. The relative levels of active Cdc42 were quantified by densitometric analyses of the immunoblots. Shown are the average values for control cells (n = 5) and cells expressing the shRNA to ARHGAP21 (n = 4). Bars, SE. (C) Shown are confocal micrographs of Vero cells labeled with an N-WASP antibody. The cells were incubated with STxB for 20 min where indicated. Bar, 10 μm. The graph shows the fraction of cells with perinuclear N-WASP as an average from three experiments counted in a blind manner (n > 50 cells per experiment). Bars, SE. The effect of STxB on N-WASP localization was significant, $p < 0.003$.

myc-Cdc42-GTP levels relative to control (Figure 8, A and B). Because we have found that both Cdc42 and ARHGAP21 affect STxB trafficking, we tested whether STxB inactivated Cdc42 in an ARHGAP21-dependent manner. We found that STxB no longer decreased myc-Cdc42-GTP levels in cells expressing an shRNA to ARHGAP21 (Figure 8B). We expected that changes in endogenous Cdc42 activity would be reflected by altered Cdc42 effector function. We tested this by examining changes in the distribution of the Cdc42 effector N-WASP in response to STxB. N-WASP contains a CRIB domain that binds to active GTP-bound Cdc42. We found that cells incubated with STxB had less perinuclear N-WASP compared with control cells (Figure 8C). A possible conclusion is that STxB activates ARHGAP21 increasing GTP hydrolysis on Cdc42 causing a decrease in downstream effector function.

ARHGAP21 and Cdc42 Are Needed for STxB-stimulated Transport of Transferrin to a Juxtanuclear Endosomal Compartment

We have found that STxB not only uses MT/dynein-dependent transport between the endosomes and Golgi apparatus, but is able to stimulate dynein-dependent transport. Specifically, we found that the MT/dynein-dependent trafficking of transferrin from early endosomes to a juxtanuclear endosome was stimulated in cells treated with STxB (Hehnly *et al.*, 2006). In this regard we tested whether ARHGAP21 and Cdc42 signaling is required for STxB-mediated changes in MT-based transport.

We confirmed that STxB caused transferrin to accumulate in a juxtanuclear endosomal compartment (Figure 9). Interestingly, STxB no longer stimulated transferrin accumulation when cells expressed Cdc42(Q61L). Transferrin remained dispersed throughout the cell. This distribution of transferrin is similar to cells without STxB and Cdc42(Q61L) (Figure 9A). Evidence that the ARHGAP21-regulated pool of Cdc42 was required for STxB effects was obtained by inhibiting ARHGAP21 expression. When STxB and transferrin were added simultaneously to cells expressing the shRNA targeting ARHGAP21, the transferrin was internalized but remained dispersed (Figure 9B). We concluded that ARHGAP21 and Cdc42 are involved both in STxB trafficking to the Golgi region and for the ability of STxB to stimulate

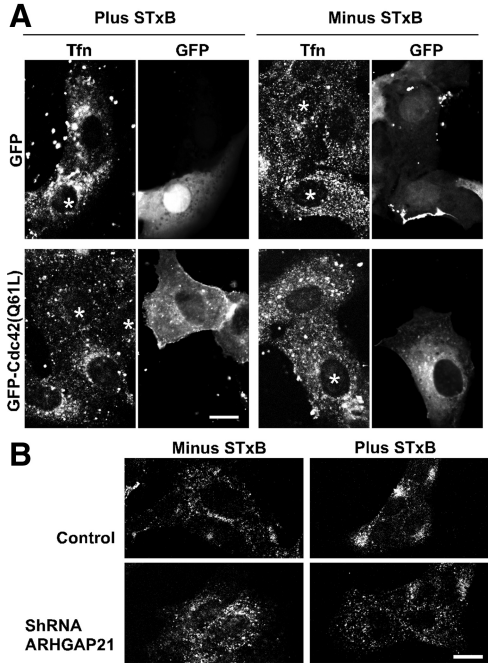

Figure 9. Cdc42(Q61L) or shARHGAP21 expression inhibits the STxB-stimulated transport of transferrin to a juxtanuclear endosomal compartment. (A) Shown are confocal micrographs of Vero cells expressing either GFP or GFP-Cdc42(Q61L) (marked with asterisks). The cells were incubated simultaneously with STxB and Alexa Fluor 647–labeled transferrin for 30 min as indicated. After 30 min, the cells were fixed and mounted for microscopy. (B) Shown is the effect of STxB treatment on Alexa Fluor 647–labeled transferrin distribution in control cells and cells stably expressing an shRNA to ARHGAP21. Bars, 10 μm.

MT/dynein mediated trafficking steps. It is likely that STxB increases the rate of dynein-dependent motility in order to facilitate its own retrograde transport through the secretory pathway.

DISCUSSION

The AB-type bacterial toxins such as Shiga toxin are remarkable in their ability to enter the cytosol by usurping the cellular trafficking machinery and undergoing retrograde transport from the cell surface to the endoplasmic reticulum. We find that Shiga toxin transport from endosomes to the juxtanuclear Golgi apparatus requires the actin cytoskeleton (Supplemental Figure S3) and dynein-dependent motility along MTs (Hehnly *et al.*, 2006). Shiga toxin not only uses cytoskeleton-dependent transport but also stimulates MT assembly and dynein-dependent motility (Hehnly *et al.*, 2006). Together, these findings imply that regulated cytoskeletal dynamics and motor protein function are necessary for efficient retrograde toxin transport. The Rho-family of GTP-binding proteins plays a central role in regulating the cytoskeleton. In this study, we find that Shiga toxin affects Cdc42 activation and that RhoA, Rac1, and Cdc42 each contribute during Shiga toxin trafficking from the cell surface to the Golgi apparatus. We find that the STxB-stimulated dynein-based transport from endosomes to the Golgi complex is regulated by a signaling pathway involving Cdc42 and the Cdc42-specific GTPase activating protein, ARHGAP21.

RhoA and Cdc42 Regulate Distinct Aspects of Shiga Toxin Transport

Some steps during Shiga toxin trafficking, such as endosome-to-Golgi transport, are cytoskeleton dependent (Figure 1 and Supplemental Figure S3; Hehnly *et al.*, 2006). Other steps, such as Golgi entry, are independent of the cytoskeleton (Mallard *et al.*, 1998). In this respect, we have examined whether Rho GTPases are required for several resolvable steps during Shiga toxin transport. We find that the initial Gb3-dependent binding of Shiga toxin to the cell surface is unaffected upon acute or long-term disruption of RhoA, Rac1, or Cdc42. This indicates that Rho function is not essential to maintain sufficient Gb3 levels on the plasma membranes. Indeed, Shiga toxin bound to cells and underwent endocytosis even upon acute inhibition of all Rho proteins using toxin B (Figure 2).

Long-term disruption of RhoA, by expression of constitutively active and dominant-negative mutants, blocked both Shiga toxin and transferrin endocytosis. This suggests that RhoA plays a general regulatory role during endocytosis and is consistent with a previously published report (Lamaze *et al.*, 1996). Long-term inhibition of Cdc42 and Rac1 had little or no effect on endocytosis. Cells expressing constitutively active or dominant-negative Cdc42 displayed severe defects in transport to the Golgi apparatus causing the toxin to remain in dispersed endosomes. Cells expressing mutant Rac1 displayed more subtle defects in STxB transport. Rac1 function may not be needed for STxB trafficking or might be complemented by another member of the Rho family.

As has been observed for other small GTPases (Wu *et al.*, 2000; Desai *et al.*, 2004; Hoppe *et al.*, 2006), we find that both constitutively active and dominant-negative mutations of RhoA and Cdc42 have inhibitory effects on STxB transport. This likely indicates that the role of these proteins during Shiga toxin trafficking requires completion of the GTP-exchange/GTP-hydrolysis cycle. Importantly, the dominant-negative and constitutively active forms of each GTPase disrupt the same trafficking step. Our observations support the conclusion that each of the Rho subfamilies regulates a distinct aspect of retrograde Shiga toxin transport.

Both Actin and MTs Are Required for Shiga Toxin's Retrograde Motility

We find that there is a cytoskeleton-dependent transport step that occurs between early endosomes and the Golgi apparatus. Using nocodazole and cytochalasin D treatments, we showed that both actin and MTs are required for Shiga toxin trafficking. The requirement for both major classes of cytoskeleton filaments could indicate that there are sequential actin- and MT/dynein-mediated motility steps. In this case, actin could either serve as a track for myosin motors or generate comet tails for actin assembly-dependent motility. Alternatively, actin could be required concurrently with dynein motors for MT-dependent transport. This latter possibility is consistent with our previous studies, indicating that Cdc42-regulated actin dynamics are necessary for the correct recruitment of dynein during vesicular transport at the Golgi apparatus (Chen *et al.*, 2005).

ARHGAP21 and Cdc42 Regulate Shiga Toxin's Dynein-mediated Transport to the Golgi Apparatus

Cdc42 mutations may influence STxB trafficking by shifting the mode of endocytosis (i.e., from nonclathrin to clathrin mediated; Kumari and Mayor, 2008). However, our previous work suggests more direct links between Cdc42 and dynein-

based motility events. We have reported that Cdc42-GTP blocks dynein recruitment in vitro (Chen *et al.*, 2005). Furthermore, inhibiting or activating Cdc42 blocks dynein-dependent ER to Golgi trafficking (Wu *et al.*, 2000; Chen *et al.*, 2005). We have now found that disrupting Cdc42 function predominantly affects endosome-to-Golgi trafficking, a step we have found to be MT- and dynein-dependent. Shiga toxin not only uses MTs for this step but also up regulates dynein-dependent motility in a manner that facilitates its own intracellular trafficking. Although it is possible that Cdc42 function during retrograde Shiga toxin transport is occurring from a distance (i.e., from the Golgi apparatus or plasma membrane), we believe it is more likely that our results reflect signaling events occurring on endosomal membranes.

Our findings regarding the effect of STxB on Cdc42 activation and the effects of Cdc42 activation on STxB trafficking suggest the following model. Shiga toxin binding or entry into cells activates the Cdc42-specific GAP, ARHGAP21 causing a decrease in the levels of GTP-bound Cdc42. Inactivation of Cdc42 relieves its inhibitory effect on dynein/microtubule-dependent motility. The increased dynein activity would facilitate the retrograde endosome-to-Golgi transport of Shiga toxin itself as well as other endocytosed proteins such as transferrin.

Rho GTPases receive input from numerous signaling pathways and function through a wide array of effector proteins. In this way, Rho proteins are able to regulate many different aspects of cell physiology. Indeed, we find that three members of the Rho family each regulate distinct aspects of retrograde transport through the secretory pathway. Signaling specificity among Rho GTPases is likely derived by directing localization and limiting effector interactions. Our finding that the specific effects of Cdc42 on dynein-dependent transport requires the function of ARHGAP21, provides important insight into how a ubiquitously-used molecular switch might direct a specific step within the secretory pathway. Further progress will likely yield additional GEFs, GAPS, and effectors that allow Rho-family proteins to regulate multiple specific aspects of membrane transport and intracellular motility.

ACKNOWLEDGMENTS

We thank Jenna McKenzie and Weidong Xu for reading the manuscript. This work was supported by the National Institutes of Health Grant GM-068674 to M.A.S.; the Dr. Ramon D. Buckley student scholarship fund, Department of Molecular Physiology and Biophysics, University of Iowa to H.A.H.; and the American Heart Association Grants 0715567Z to H.A.H. and 0950167G to M.A.S.

REFERENCES

Aktories, K., Schmidt, G., and Just, I. (2000). Rho GTPases as targets of bacterial protein toxins. Biol. Chem. *381*, 421–426.

Bujny, M. V., Popoff, V., Johannes, L., and Cullen, P. J. (2007). The retromer component sorting nexin-1 is required for efficient retrograde transport of Shiga toxin from early endosome to the trans Golgi network. J. Cell Sci. *120*, 2010–2021.

Chen, J. L., Fucini, R. V., Lacomis, L., Erdjument-Bromage, H., Tempst, P., and Stamnes, M. (2005). Coatomer-bound Cdc42 regulates dynein recruitment to COPI vesicles. J. Cell Biol. *169*, 383–389.

Chiang, S. H., Baumann, C. A., Kanzaki, M., Thurmond, D. C., Watson, R. T., Neudauer, C. L., Macara, I. G., Pessin, J. E., and Saltiel, A. R. (2001). Insulin-stimulated GLUT4 translocation requires the CAP-dependent activation of TC10. Nature *410*, 944–948.

de Toledo, M., Senic-Matuglia, F., Salamero, J., Uze, G., Comunale, F., Fort, P., and Blangy, A. (2003). The GTP/GDP cycling of rho GTPase TCL is an essential regulator of the early endocytic pathway. Mol. Biol. Cell *14*, 4846–4856.

Deroanne, C. F., Hamelryckx, D., Ho, T. T., Lambert, C. A., Catroux, P., Lapiere, C. M., and Nusgens, B. V. (2005). Cdc42 downregulates MMP-1 expression by inhibiting the ERK1/2 pathway. J. Cell Sci. *118*, 1173–1183.

Desai, L. P., Aryal, A. M., Ceacareanu, B., Hassid, A., and Waters, C. M. (2004). RhoA and Rac1 are both required for efficient wound closure of airway epithelial cells. Am J. Physiol. Lung Cell Mol. Physiol. *287*, L1134–L1144.

Desch, K. C., and Motto, D. G. (2007). Thrombotic thrombocytopenic purpura in humans and mice. Arterioscler Thromb. Vasc. Biol. *27*, 1901–1908.

Dubois, T., Paleotti, O., Mironov, A. A., Fraisier, V., Stradal, T. E., De Matteis, M. A., Franco, M., and Chavrier, P. (2005). Golgi-localized GAP for Cdc42 functions downstream of ARF1 to control Arp2/3 complex and F-actin dynamics. Nat. Cell Biol. *7*, 353–364.

Etienne-Manneville, S., and Hall, A. (2002). Rho GTPases in cell biology. Nature *420*, 629–635.

Falguieres, T., Mallard, F., Baron, C., Hanau, D., Lingwood, C., Goud, B., Salamero, J., and Johannes, L. (2001). Targeting of Shiga toxin B-subunit to retrograde transport route in association with detergent-resistant membranes. Mol. Biol. Cell *12*, 2453–2468.

Fuchs, E., Haas, A. K., Spooner, R. A., Yoshimura, S., Lord, J. M., and Barr, F. A. (2007). Specific Rab GTPase-activating proteins define the Shiga toxin and epidermal growth factor uptake pathways. J. Cell Biol. *177*, 1133–1143.

Fucini, R. V., Chen, J. L., Sharma, C., Kessels, M. M., and Stamnes, M. (2002). Golgi vesicle proteins are linked to the assembly of an actin complex defined by mAbp1. Mol. Biol. Cell *13*, 621–631.

Girod, A., Storrie, B., Simpson, J. C., Johannes, L., Goud, B., Roberts, L. M., Lord, J. M., Nilsson, T., and Pepperkok, R. (1999). Evidence for a COP-I-independent transport route from the Golgi complex to the endoplasmic reticulum. Nat. Cell Biol. *1*, 423–430.

Hall, A. (2005). Rho GTPases and the control of cell behaviour. Biochem. Soc. Trans. *33*, 891–895.

Hehnly, H., Sheff, D., and Stamnes, M. (2006). Shiga toxin facilitates its retrograde transport by modifying microtubule dynamics. Mol. Biol. Cell *17*, 4379–4389.

Hoppe, S., Schelhaas, M., Jaeger, V., Liebig, T., Petermann, P., and Knebel-Morsdorf, D. (2006). Early herpes simplex virus type 1 infection is dependent on regulated Rac1/Cdc42 signalling in epithelial MDCKII cells. J. Gen. Virol. *87*, 3483–3494.

Johannes, L., and Popoff, V. (2008). Tracing the retrograde route in protein trafficking. Cell *135*, 1175–1187.

Kumari, S., and Mayor, S. (2008). ARF1 is directly involved in dynamin-independent endocytosis. Nat. Cell Biol. *10*, 30–41.

Lamaze, C., Chuang, T. H., Terlecky, L. J., Bokoch, G. M., and Schmid, S. L. (1996). Regulation of receptor-mediated endocytosis by Rho and Rac. Nature *382*, 177–179.

Lauvrak, S. U., Torgersen, M. L., and Sandvig, K. (2004). Efficient endosome-to-Golgi transport of Shiga toxin is dependent on dynamin and clathrin. J. Cell Sci. *117*, 2321–2331.

Lauvrak, S. U., Walchli, S., Iversen, T. G., Slagsvold, H. H., Torgersen, M. L., Spilsberg, B., and Sandvig, K. (2006). Shiga toxin regulates its entry in a Syk-dependent manner. Mol. Biol. Cell *17*, 1096–1109.

Lingwood, C. A. (1993). Verotoxins and their glycolipid receptors. Adv. Lipid Res. *25*, 189–211.

Luna, A., Matas, O. B., Martinez-Menarguez, J. A., Mato, E., Duran, J. M., Ballesta, J., Way, M., and Egea, G. (2002). Regulation of protein transport from the Golgi complex to the endoplasmic reticulum by CDC42 and N-WASP. Mol. Biol. Cell *13*, 866–879.

Mallard, F., Antony, C., Tenza, D., Salamero, J., Goud, B., and Johannes, L. (1998). Direct pathway from early/recycling endosomes to the Golgi apparatus revealed through the study of shiga toxin B-fragment transport. J. Cell Biol. *143*, 973–990.

Mallard, F., Tang, B. L., Galli, T., Tenza, D., Saint-Pol, A., Yue, X., Antony, C., Hong, W., Goud, B., and Johannes, L. (2002). Early/recycling endosomes-to-TGN transport involves two SNARE complexes and a Rab6 isoform. J. Cell Biol. *156*, 653–664.

Malyukova, I., Murray, K. F., Zhu, C., Boedeker, E., Kane, A., Patterson, K., Peterson, J. R., Donowitz, M., and Kovbasnjuk, O. (2009). Macropinocytosis in Shiga toxin 1 uptake by human intestinal epithelial cells and transcellular transcytosis. Am J. Physiol. Gastrointest. Liver Physiol. *296*, G78–G92.

McKenzie, J., Johannes, L., Taguchi, T., and Sheff, D. (2009). Passage through the Golgi is necessary for Shiga toxin B subunit to reach the endoplasmic reticulum. FEBS J. *276*, 1581–1595.

Menetrey, J., Perderiset, M., Cicolari, J., Dubois, T., Elkhatib, N., El Khadali, F., Franco, M., Chavrier, P., and Houdusse, A. (2007). Structural basis for ARF1-mediated recruitment of ARHGAP21 to Golgi membranes. EMBO J. *26*, 1953–1962.

Monier, S., Jollivet, F., Janoueix-Lerosey, I., Johannes, L., and Goud, B. (2002). Characterization of novel Rab6-interacting proteins involved in endosome-to-TGN transport. Traffic *3*, 289–297.

Naslavsky, N., McKenzie, J., Altan-Bonnet, N., Sheff, D., and Caplan, S. (2009). EHD3 regulates early-endosome-to-Golgi transport and preserves Golgi morphology. J. Cell Sci. *122*, 389–400.

O'Loughlin, E. V., and Robins-Browne, R. M. (2001). Effect of Shiga toxin and Shiga-like toxins on eukaryotic cells. Microbes Infect. *3*, 493–507.

Obata, F., Tohyama, K., Bonev, A. D., Kolling, G. L., Keepers, T. R., Gross, L. K., Nelson, M. T., Sato, S., and Obrig, T. G. (2008). Shiga toxin 2 affects the central nervous system through receptor globotriaosylceramide localized to neurons. J. Infect. Dis. *198*, 1398–1406.

Obrig, T. G., Moran, T. P., and Colinas, R. J. (1985). Ribonuclease activity associated with the 60S ribosome-inactivating proteins ricin A, phytolaccin and Shiga toxin. Biochem. Biophys. Res. Commun. *130*, 879–884.

Pfaffl, M. W. (2001). A new mathematical model for relative quantification in real-time RT-PCR. Nucleic Acids Res. *29*, e45.

Popoff, V., Mardones, G. A., Tenza, D., Rojas, R., Lamaze, C., Bonifacino, J. S., Raposo, G., and Johannes, L. (2007). The retromer complex and clathrin define an early endosomal retrograde exit site. J. Cell Sci. *120*, 2022–2031.

Proulx, F., Seidman, E. G., and Karpman, D. (2001). Pathogenesis of Shiga toxin-associated hemolytic uremic syndrome. Pediatr. Res. *50*, 163–171.

Romer, W., *et al.* (2007). Shiga toxin induces tubular membrane invaginations for its uptake into cells. Nature *450*, 670–675.

Sabharanjak, S., Sharma, P., Parton, R. G., and Mayor, S. (2002). GPI-anchored proteins are delivered to recycling endosomes via a distinct cdc42-regulated, clathrin-independent pinocytic pathway. Dev. Cell *2*, 411–423.

Saenz, J. B., Sun, W. J., Chang, J. W., Li, J., Bursulaya, B., Gray, N. S., and Haslam, D. B. (2009). Golgicide A reveals essential roles for GBF1 in Golgi assembly and function. Nat. Chem. Biol. *5*, 157–165.

Sandvig, K., and van Deurs, B. (2000). Entry of ricin and Shiga toxin into cells: molecular mechanisms and medical perspectives. EMBO J. *19*, 5943–5950.

Sandvig, K., and van Deurs, B. (2002). Transport of protein toxins into cells: pathways used by ricin, cholera toxin and Shiga toxin. FEBS Lett. *529*, 49–53.

Tai, G., Lu, L., Johannes, L., and Hong, W. (2005). Functional analysis of Arl1 and golgin-97 in endosome-to-TGN transport using recombinant Shiga toxin B fragment. Methods Enzymol. *404*, 442–453.

Tai, G., Lu, L., Wang, T. L., Tang, B. L., Goud, B., Johannes, L., and Hong, W. (2004). Participation of the syntaxin 5/Ykt6/GS28/GS15 SNARE complex in transport from the early/recycling endosome to the trans-Golgi network. Mol. Biol. Cell *15*, 4011–4022.

Takenouchi, H., Kiyokawa, N., Taguchi, T., Matsui, J., Katagiri, Y. U., Okita, H., Okuda, K., and Fujimoto, J. (2004). Shiga toxin binding to globotriaosyl ceramide induces intracellular signals that mediate cytoskeleton remodeling in human renal carcinoma-derived cells. J. Cell Sci. *117*, 3911–3922.

Torgersen, M. L., Lauvrak, S. U., and Sandvig, K. (2005). The A-subunit of surface-bound Shiga toxin stimulates clathrin-dependent uptake of the toxin. FEBS J. *272*, 4103–4113.

Torgersen, M. L., Walchli, S., Grimmer, S., Skanland, S. S., and Sandvig, K. (2007). Protein kinase Cdelta is activated by Shiga toxin and regulates its transport. J. Biol. Chem. *282*, 16317–16328.

Walchli, S., Skanland, S. S., Gregers, T. F., Lauvrak, S. U., Torgersen, M. L., Ying, M., Kuroda, S., Maturana, A., and Sandvig, K. (2008). The mitogen-activated protein kinase p38 links Shiga toxin-dependent signaling and trafficking. Mol. Biol. Cell *19*, 95–104.

Wilcke, M., Johannes, L., Galli, T., Mayau, V., Goud, B., and Salamero, J. (2000). Rab11 regulates the compartmentalization of early endosomes required for efficient transport from early endosomes to the trans-golgi network. J. Cell Biol. *151*, 1207–1220.

Wu, W. J., Erickson, J. W., Lin, R., and Cerione, R. A. (2000). The gamma-subunit of the coatomer complex binds Cdc42 to mediate transformation. Nature *405*, 800–804.

Yoshino, A., *et al.* (2005). tGolgin-1 (p230, golgin-245) modulates Shiga-toxin transport to the Golgi and Golgi motility towards the microtubule-organizing centre. J. Cell Sci. *118*, 2279–2293.